

# EFFECT OF X-RAYS ON THE MECHANICAL PROPERTIES OF ALUMINIZED FEP TEFLON®

James R. Gaier  
NASA Lewis Research Center, Cleveland, OH 44135

Michael R. Brinkmeier and Elizabeth M. Gaier  
Manchester College, North Manchester, IN 46962

## ABSTRACT

Pieces of the multilayer insulation (MLI) that is integral to the thermal control of the Hubble Space Telescope (HST) have been returned by two servicing missions after 3.6 and 6.8 years in orbit. They reveal that the outer layer, which is made from 5 mil (0.13 mm) thick aluminized fluorinated ethylenepropylene (FEP) Teflon®, has become severely embrittled. Although possible agents of this embrittlement include electromagnetic radiation across the entire solar spectrum, trapped particle radiation, atomic oxygen, and thermal cycling, intensive investigations have not yielded unambiguous causes. Previous studies utilizing monoenergetic photons in the 69-1900 eV range did not cause significant embrittlement, even at much higher doses than were experienced by the HST MLI. Neither did x-rays in the 3 to 10 keV range generated in a modified electron beam evaporator. An antidotal aluminized FEP sample that was exposed to an intensive dose from unfiltered Mo x-ray radiation from a rotating anode generator, however, did show the requisite embrittlement. Thus, a study was undertaken to determine the effects of x-ray exposure on the embrittlement of aluminized FEP in hopes that it might elucidate the HST MLI degradation mechanism. Tensile specimens of aluminized 5 mil thick FEP were exposed to a constant fluence of unfiltered x-ray radiation from a Mo target whose maximum energy ranged from 20-60 kV. Other samples were annealed, thermally cycled (100×) between 77-333 K, or cycled and irradiated. Tensile tests and density measurements were then performed on the samples. Only the samples which had been irradiated had the drastically reduced elongation-to-break, characteristic of the HST samples. Thermal cycling may accelerate the embrittlement, but the effect was near the scatter in the measurements. Annealing and thermal cycling had no apparent effect. Only the samples which had been irradiated and annealed showed significant density increases, likely implicating polymer chain scission and annealing.

## INTRODUCTION

Effective thermal control of spacecraft is essential to their long-term operational success. To that end, strategies have been developed which reflect the heat load of the sun and yet emit infrared in the shadow. One of the most effective strategies is multi-layer insulation (MLI) in which there are several reflective layers (such as double sided aluminized Kapton®) with a transparent emitting layer on the outer surface (such as single sided silvered or aluminized FEP Teflon®). These materials are used extensively on the Hubble Space Telescope (HST).

The HST was first deployed on April 25, 1990 at an altitude of 614 km. On December 4, 1993 it was serviced to correct the optical flaw in its primary mirror and to upgrade its electronics. Servicing mission 1 (SM1) retrieved parts of the MLI which had been exposed to the environment for 3.6 years. This included covers on two magnetometer electronics boxes which jutted out from the surface of the light shield. Different sides of the boxes were exposed to slightly different environments with solar exposures ranging from 4,500 to 16,700 equivalent sun hours (ESH). Surprisingly, cracks which extended completely through the surface of the metallized FEP were observed.<sup>1</sup> This cracking lead to an investigation into its possible causes.

When the HST was serviced a second time (SM2) on February 15, 1997, the damage to the MLI was markedly worse. This was in spite of the fact that the HST had encountered a substantially lower flux of atomic oxygen since SM1. Cracks in the FEP layer of the MLI that were tens of cm long and curled to expose the inner layers were clearly visible to the astronauts (Figure 1). The most heavily damaged sections of the MLI were removed and covered with patches. However, it was evident that the damage was increasing. NASA established a failure review board to determine the cause of the damage, predict the condition of the MLI at the next servicing mission, and to recommend MLI replacement materials for the third servicing mission, scheduled for 1999.

The orbital environment of the HST includes electromagnetic radiation across the entire solar spectrum, high energy electron and protons that have been trapped in the Earth's magnetic field, thermal cycles ranging from -100 to +50 °C on the solar facing surfaces, and from -200 to -10 °C on the anti-solar surfaces, and energetic atomic oxygen, all of which are candidates to be agents of the degradation. Despite three years of intensive study by researchers throughout NASA, no unambiguous cause of the FEP failure has been identified.<sup>1,2,3</sup> To replicate the chemical, thermal, and radiation environment experienced by HST has proved daunting, and

to date no tests under realistic simulation conditions have been able to replicate the extent of damage to the material. It is the object of this study to study one aspect of the HST environment, x-ray exposure, and to determine how it affects the mechanical properties of FEP, in the hopes of beginning to unravel the complex web of interactions.

That the x-ray environment might be involved was first suggested by Milintchouk, et al.<sup>4</sup> They argued that ultraviolet radiation would only alter the surface, because its penetration depth is so low. Although many x-ray have such a large penetration depth that they would not deposit sufficient energy to cause damage, photons in the soft x-ray regions (0.1 to 10 keV) have penetration depths similar to the thickness of the materials (0.13 mm or 0.005 in). The source of these soft x-rays would be solar flares. HST saw more solar flares than the Long Duration Exposure Facility (LDEF), which might explain why the HST MLI was so much more heavily damaged than similar materials that were exposed on LDEF, which had logged more hours in space.<sup>4</sup> Previous studies using monochromatic radiation in the range of 69 to 1900 eV showed little or no embrittlement of the FEP even at doses greatly exceeding that experienced by HST.<sup>3</sup> Embrittlement was also not seen when mission level doses of x-rays in the 3 to 10 keV generated by a modified electron beam evaporator was used.<sup>2</sup> Discoloration of some of the samples raised issues about whether there might also be charged particles or heating in these tests as well as x-ray exposure.

For the initial tests to see whether x-rays would embrittle 5 mil thick aluminized FEP, x-rays were generated in a rotating anode generator with an excitation voltage of 50 kV, an excitation current of 60 mA, and an exposure time of 1 hour. Although this sample was not tensile tested, it was not obviously embrittled. The FEP sample returned from SM2 showed considerable surface cracking (Figure 2), and though this may have been caused by the flattening out of the curled sample rather than the damage *per se*, it was not seen in the irradiated sample. When FEP was irradiated for 5 hours (50 kV, 60 mA), the texture of the irradiated area changed it from a specular to a diffuse reflector. When this sample was kinked with two pairs of forceps, there was an audible snap. Photomicrographs showed a brittle failure with sharp edges which ends abruptly at the edge of the exposed region (Figure 3). To achieve the same photon fluence, but at lower energy, a sample was exposed to x-rays generated at 20 kV and 60 mA for 31.25 hr. After this exposure, all of the aluminum appeared to be removed from the irradiated part of the sample and a large crack, as well as a few secondary cracks, developed across the entire length of the irradiated region of the sample when it was gently removed from the sample holder (Figure 4). In addition, drops of an unidentified liquid began to appear on the surface of the FEP. The drops, which increased with time, formed at the cracks (Figure 5). SEM photos of the crack surfaces indicate a thin surface layer ( $\approx 5 \mu\text{m}$ ), a brittle failure region (20 - 120  $\mu\text{m}$ ), and a region of scalloped structures (0 - 120  $\mu\text{m}$ ) (Figure 6). At this point, a test program was designed that would quantify the brittleness of the material using elongation-to-failure in tension as an indicator.

## METHODS AND MATERIALS

Aluminized FEP Teflon® of 0.013 mm (0.005 in) thickness was purchased from Sheldahl Inc. (Northfield, MN) which has supplied the original HST MLI material. Tensile dog-bone specimens were punched out using an ASTM 638-95 Type V Punch and an Arbor press. The width of the narrow portion of the dog-bone was 3.18 mm and the gauge length was 9.53 mm. Specimens were punched out both parallel and perpendicular to the direction which the FEP was machined.

Elongation-to-failure was chosen as the critical criterion to measure. Samples recovered from HST had elongation-to-failure so low as to not be measurable, while under similar conditions pristine FEP has an elongation-to-failure of about 200 percent. A computer controlled tensile tester was designed and assembled onsite<sup>5</sup> based on a 5 lb load cell (Sensotech Model 11). The tensile tester and grips were designed and optimized specifically for these samples. The test procedure was based on the ASTM standard. Since FEP is particularly susceptible to creep, all dog-bones were strained at a constant rate of 0.0210 cm/sec (0.00827 in/sec). Stress-strain curves were analyzed and ultimate tensile strength, tensile modulus, and elongation-to-failure were recorded for each sample.

The source of the x-ray exposure was a Rigaku Rotaflex BEH rotating anode source equipped with a Mo target. The x-rays passed through a 0.40 mm thick Be window and 1.90 cm of air before striking the sample. The excitation potential across the anode was varied from 20 to 60 kV, resulting in Bremsstrahlung with a maximum photon energy ranging from 20 to 60 keV. There is also a resonant energy spike at the  $K_{\alpha}$  energy for Mo of 17.4 keV superimposed on the Bremsstrahlung. The approximate shape and spectral variation less the Mo  $K_{\alpha}$  spike is shown in Figure 7.<sup>6</sup> Since the photon intensity is also a function of excitation potential, the time must be adjusted if the total fluence from trial to trial is to remain constant. The assumption was made that the photon intensity varied as the square of the excitation potential and linearly with the excitation current.<sup>5</sup> X-ray exposure conditions are shown in Table I.

The integrated intensity of the x-ray beam was determined using an AXUV detector (International Radiation Detectors, Torrence, CA) operating with a 7.5 volt bias voltage. This detector is sensitive to radiation from 10 to at least 4000 eV. Detector current was measured for values of the excitation potential ranging from 20 to 60 kV, and excitation currents from 10 to 70 mA. The dark current was three orders of magnitude below the lowest value for the detector current and so was neglected. Over this energy range the x-ray intensity varied linearly with both excitation potential and current as is shown in Figure 8.

Another characteristic of the FEP on HST that changed during its space exposure was its density. Thus, the density of several samples was measured using a calibrated density gradient technique which has been described in detail elsewhere.<sup>7</sup> The density solvents used were carbon tetrachloride ( $\text{CCl}_4$ ) which has a density of 1.594 g/cm<sup>3</sup>, and bromoform ( $\text{CHBr}_3$ ) which has a density of 2.899 g/cm<sup>3</sup>. Neither of these would be expected to interact significantly with the FEP.

The particular SM2 sample tested had rolled up in cylinder with a diameter of several mm and was not in good thermal contact with HST (top tear shown in Figure 1). Additionally, the reflective aluminum layer was outward facing, and the emissive FEP layer was inward facing. Calculations indicate it had likely reached temperatures as high as 200 °C.<sup>8</sup> Thus, it is possible that the high temperatures seen by this particular sample were responsible for the increased embrittlement and density. So several samples were annealed in an oven at 200 °C in air for times ranging from 1.0 to 96.0 hr.

In addition to the high temperatures seen by that particular sample, the entire HST is thermally cycled as it travels in and out of the earth's shadow. Calculations have estimated thermal swings between -100 and +50 °C.<sup>2</sup> This would take the FEP through the lower of its two second order phase transitions, which occurs at -85 °C (the other occurs at +85 °C).<sup>9</sup> Thus, it was thought important to cycle some of the test specimens to temperatures below and above that phase transition. This was done by attaching them to a sample holder by pinching them in the very end of the samples, well away from the grip and test sections. The sample were then submerged in liquid nitrogen (-196 °C) for 30 s, and then placed in an incubator maintained at 60 °C for 330 s. This cycling was repeated for 100 cycles, well below the 21,000 thermal cycles experienced by HST<sup>2</sup>, but perhaps enough to see at least the beginning of degradation. Samples were included which had been previously exposed to the x-rays, and others were subsequently exposed to the x-rays.

## RESULTS AND DISCUSSION

The first issue to be addressed was whether the machine direction was correlated with the tensile properties. To this end ten samples of the aluminized FEP were cut parallel to, and ten perpendicular to the machine direction. The elongation to failure parallel to the machine direction was  $196 \pm 9$  percent, and that for samples cut perpendicular was  $187 \pm 11$  percent. These values were judged to be statistically insignificant by Student's t test, so a combined pristine elongation-to-failure of  $192 \pm 11$  percent was used throughout the rest of the study. For comparison, FEP returned from HST SM1 had an elongation-to-failure of 41 percent.<sup>2</sup>

The effect of annealing time at 200 °C on the percent elongation-to-failure is shown in Figure 9. Only one or two samples were tested at each anneal temperature, so the mean  $\pm$  standard deviation for the pristine samples are superimposed on this figure. The least squares fit through the data has a slope of 0.014 percent elongation per hour, well within the error of the measurements, and in the direction of decreasing brittleness. All of the data lie within one standard deviation of the mean of the pristine value, so there is no indication that annealing at 200 °C for as long as 96 hr embrittles the FEP.

The samples that were thermal cycled had an elongation-to-failure of  $195 \pm 6$  percent. Thus there was no effect on the elongation-to-failure for thermal cycling at the level of 100 thermal cycles from -196 to +50 °C. HST was exposed to about 40,000 thermal cycles between launch and SM2. The fraction of degradation seen in 100 cycles would be dependent on the degradation kinetics. If 40,000 cycles or less caused a 200 percent change in elongation-to-failure in the HST MLI, and the degradation is linear, then 100 cycles might be expected to increase the elongation-to-failure by 0.5 percent, well within the error of the measurement. If, however, the degradation is exponential, then the elongation-to-failure would be expected to be about 85 percent. Since no degradation was observed, that puts limits on the extent of degradation attributable to thermal cycling alone.

Figure 10 presents the effect of x-ray exposure on the percent elongation-to-failure. All of these samples had significantly lower percent elongation-to-failure than the pristine value. In the exposure region where the maximum energy was 60 keV, the average percent elongation-to-failure dropped by an order of magnitude to  $27 \pm 6$  percent. In the exposure regions where the maximum photon energy was 40 keV elongation-to-failure was  $5 \pm 3$  percent. At a maximum photon energy of 20 keV, the decrease was  $2.0 \pm 1.3$  percent, a full two orders of magnitude less than the pristine value. FEP exposed to Mo K $\alpha$  x-rays (17.4 keV) generated using a graphite monochromator for about 24 hours had an elongation to failure of 206 percent, well within the pristine range.

The convolution of the spectrum emitted by the x-ray source and that absorbed by the FEP reveals that there is only a limited overlap region. Figure 11 compares the spectral fluence of the photons absorbed by the 20 kV and the 60 kV tests. It can be seen in this plot that the 20 kV tests resulted in much higher fluence of photons in the 3 to 15 keV region where FEP is susceptible to through-thickness damage. It also illustrates why the Mo characteristic radiation (17.4 keV) did not damage the FEP. An independent analysis by Banks et al. from a the electron beam x-ray generator which was run at 10 kV concludes that the 3-10 keV photons would be capable of inflicting the most damage.<sup>2</sup> Unlike this work, their high energy cut-off (10 keV) was dictated by the maximum energy of their x-ray source.

The fluence of x-rays being generated by the x-ray source over the experimental times was about  $10^5$  J/m<sup>2</sup>. This is three orders of magnitude higher than the fluences estimated for HST's exposure at SM2, which was about 250 J/m<sup>2</sup>.<sup>7</sup> Although the damage was more extensive in these tests than in the HST samples, antidotal tests indicated that there was minimal damage when FEP was exposed at equal fluence. Thus, it is not claimed that x-rays within the 3 to 15 keV region are solely responsible for the damage in the HST MLI. Rather, these tests indicate that there is a similar damage mechanism, probably polymer chain scission, at work in both instances.

The synergistic effects of soft x-ray exposure and thermal cycling were investigated both by thermal cycling samples and then exposing them to x-rays, and by exposing them to x-rays and then thermal cycling them. The results, shown in Table II, may indicate that thermal cycling has a small effect on the elongation-to-failure of these materials. The numbers of samples were small (3 to 4) and the results showed decreases near the scatter of the data. But Banks, et al., have also reported that more extensive thermal cycling may be implicated in the MLI degradation on HST, though the effect appears to be minor.<sup>2</sup>

The results of the density measurements are shown in Table III. The samples returned from the magnetometer shield during SM1 showed no increase in density over pristine (both at  $2.141 \pm 0.003$  g/cm<sup>3</sup>). The density of four samples were measured with solar exposure ranging from 4,500 to 16,700 equivalent sun hours, but they all had the same density. However, the density of the sample returned from SM2 was  $2.184 \pm 0.003$  g/cm<sup>3</sup>. This particular FEP sample was removed from a place on the MLI that had split and coiled up into a tight spiral with a radius of only a few mm. Calculation carried out at NASA Goddard Space Flight Center indicate that temperatures on this section may have reached as high as 200 °C.<sup>7</sup> It has been suggested by de Groh *et al.* that the density increase is caused by polymer chain scission within the FEP, followed by annealing, which allows the shortened chains to pack more densely.<sup>10</sup> The results of this study confirm those of de Groh. Merely annealing the FEP increased its density by as much as 1.0 percent. Irradiating the FEP far beyond the levels experienced by HST increased its density by 0.7 percent. However, if the FEP is first exposed to soft x-rays and then annealed, its density increases by nearly 2.7 percent. This increase in the irradiated and annealed FEP density supports chain scission as a degradation mechanism.

The percent crystallinity of the sample can be determined from the density.<sup>11</sup> It can be seen that the crystallinity is a strong function of the density. Thus, though there is a range of densities of only 2 percent in these samples, it corresponds to nearly a 20 percent range in the crystallinity. Thus even small density changes support a chain scission mechanism.

## CONCLUSIONS

A study has been carried out to study the effects of x-ray exposure of FEP Teflon on its brittle failure, as characterized by its elongation-to-failure. Elongation-to-failure was unchanged for machine direction, annealing to 200 °C for up to 96 hr, and up to 100 thermal cycles between -196 and 50 °C. However, it fell from  $192 \pm 11$  percent to  $27 \pm 6$  percent when exposed to Bremsstrahlung with a maximum photon energy of 60 keV,  $5 \pm 3$  percent at 40 keV, and to  $2.0 \pm 1.3$  percent at 20 keV. Modeling indicates that 5 mil (0.13 mm) thick FEP would be most sensitive to through thickness cracking when exposed to radiation from 3 to 15 keV. Lower energy radiation will be absorbed near the surface, and higher energy radiation will pass through with little interaction. Our experimental data confirm this model. The elongation-to-failure of samples irradiated by 20 keV maximum energy photons was an order of magnitude less than those irradiated by 60 keV maximum photons. Thermal cycling (100×) may accelerate the embrittlement when combined with irradiation, though the effect was near the scatter in the measurements. The density of FEP increases by about 1.0 percent when annealed at 200 °C for 24 hour. Irradiation with x-rays increases the density by about 0.7 percent. However, if the sample is irradiated and then annealed its density increases by about 2.7 percent. This observation supports a degradation mechanism where x-rays in the 3 to 15 keV range can be absorbed, causing chain scission and subsequent degradation of the flexibility of the polymer. If the polymer is then heated, the newly formed shorter chains can rearrange more efficiently which increases the crystallinity and so also the density.

degradation of the flexibility of the polymer. If the polymer is then heated, the newly formed shorter chains can rearrange more efficiently which increases the crystallinity and so also the density.

This study was motivated by the degradation of the HST multi-layer insulation. It has shown that the embrittlement of FEP to the extent observed on the MLI could be caused by scission of the polymer chains. It is not likely that x-rays in the 3 to 15 keV range are the sole agents of the degradation, since the fluences used in this study were three orders of magnitude larger than those calculated to be present on HST, though they may be a significant contributor. This might especially be the case if the free radicals which are formed during the chain scission persist for very long periods of time and propagate. There are, however, other agents within the HST environment that may cleave the polymer chains and lead to similar degradation.

## ACKNOWLEDGMENTS

The authors would like to thank B.A. Banks, J. A. Dever, and K.K. de Groh of the NASA Lewis Research Center for their helpful discussions during the course of this work, and A. Jalics of Cleveland State University and R. Hall of Saint Mary's College for tensile data used in the pristine FEP analysis. E.M.G. gratefully acknowledges the support of the NASA Lewis Research Center under Cooperative Agreement NCC3-317.

## REFERENCES

- 1) T.M. Zuby, K.K. de Groh, and D.C. Smith, "Degradation of FEP Thermal Control Materials Returned from the Hubble Space Telescope", NASA Technical Memorandum 104627 (1995).
- 2) B.A. Banks, K.K. de Groh, T.J. Stueber, and E.A. Sechkar, "Ground Laboratory Soft X-Ray Durability Evaluation of Aluminized Teflon FEP Thermal Control Insulation", NASA Technical Memorandum 207914 (1998).
- 3) J.A. Dever, J.A. Townsend, J.R. Gaier, and A.I. Jalics, "Synchrotron VUV and Soft X-Ray Radiation Effects on Aluminized Teflon FEP", Materials and Process Affordability: Keys to the Future 43(1) (Society for the Advancement of Materials and Process Engineering, Covina, CA, 1998) pp. 616-628.
- 4) A. Milintchouk, M. Van Eesbeek, F. Levadou, and T. Harper, "Influence of X-Ray Solar Flare Radiation on Degradation of Teflon in Space", *J. Spacecraft and Rockets*, 34(4) (1997) 542.
- 5) Designed and built by T.J. Stueber, M.J. Forkapa, and E.A. Sechkar, NYMA, Cleveland, OH.
- 6) B.D. Cullity, Elements of X-Ray Diffraction, 2nd Ed. (Addison-Wesley Publishing Company, Inc., Reading, MA, 1978).
- 7) J.R. Gaier, and M.E. Slabe, "Density of Graphite Fibers", *Carbon* 34(2), 1990, pp. 1-15.
- 8) J.A. Townsend, P.A. Hansen, J.A. Dever, and J.J. Triolo, "Analysis of Retrieved Hubble Space Telescope Thermal Control Materials", Materials and Process Affordability: Keys to the Future 43(1) (Society for the Advancement of Materials and Process Engineering, Covina, CA, 1998) pp. 582-593.
- 9) Tetrafluoroethylene Polymers, Vol 13, DuPont, p. 657.
- 10) K.K. de Groh, J.R. Gaier, R. Hall, and M.J. Norris, M. Espe and D.Cato, "Effects of Heating on Teflon FEP Thermal Control Material from the Hubble Space Telescope," in preparation, 1998.
- 11) Teflon Fluorocarbon Resins: Mechanical Design Data - DuPont Product Information.

**Table I -- X-Ray Exposure Conditions**

Excitation Potential kV	Excitation Current mA	Time hr
20	70	17.89
40	70	7.94
60	70	1.98

**Table II -- Thermal Cycling + X-Ray Radiation**

Thermal Cycling	X-Ray Exposure	% Elongation to Failure
none	none	192 ± 11
100×	none	195 ± 6
none	60 keV	27 ± 6
100× before	60 keV	18 ± 0.5
none	20 keV	2.0 ± 1.3
100× after	20 keV	1.5 ± 0.9

**Table III -- Density of Alumized 5 mil FEP  
Under Various Conditions**

Material	Density g/cm <sup>3</sup>	Crystallinity percent
pristine	2.141	50.6
SM1	2.141	50.6
annealed 1 hr	2.149	53.2
60 kV x-rays	2.157	55.9
annealed 3 hr	2.159	56.5
annealed 5 hr	2.160	56.8
annealed 7 hr	2.160	56.8
annealed 24 hr	2.163	57.8
SM2	2.184	64.7
x-ray + 1 hr ann	2.193	67.7
x-ray + 3 hr ann	2.195	68.4
x-ray + 5 hr ann	2.197	69.0
x-ray + 7 hr ann	2.198	69.4



**Figure 1--** Damaged FEP outer layer in multi-layer insulation of Hubble Space Telescope.

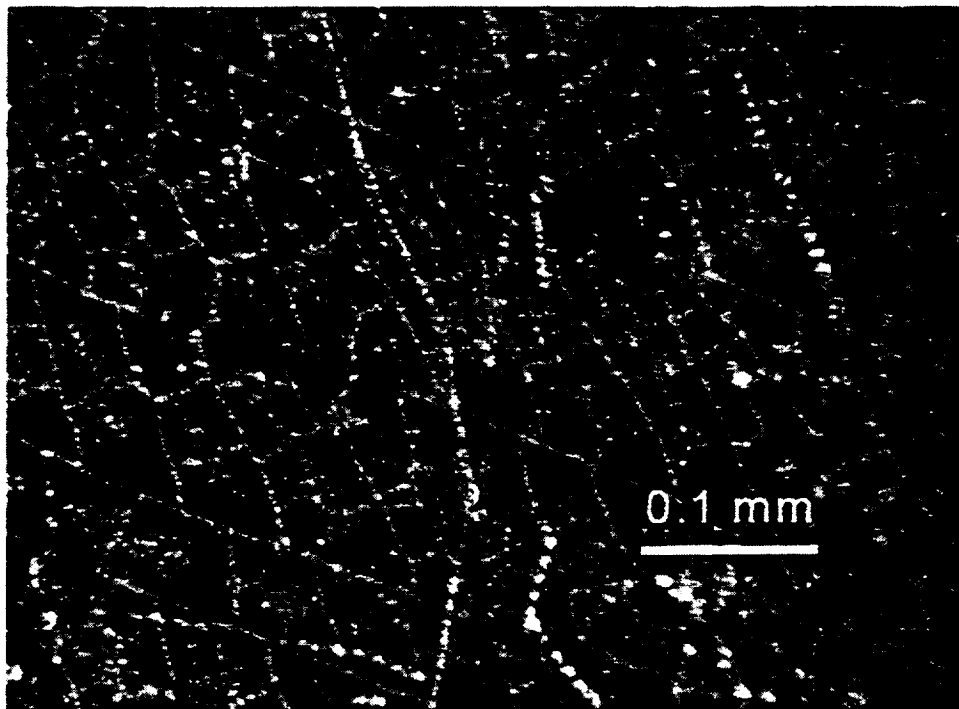


**Figure 2 --** Surface cracks in FEP from MLI returned from HST during SM2.

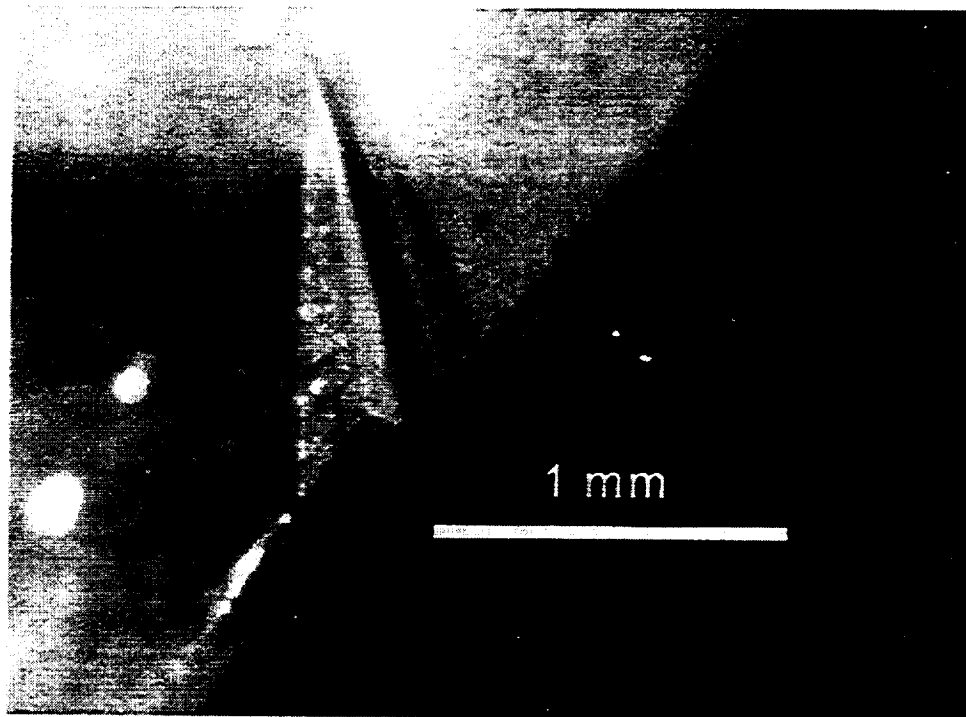


**Figure 3 – Brittle fracture in FEP after x-ray irradiation.**

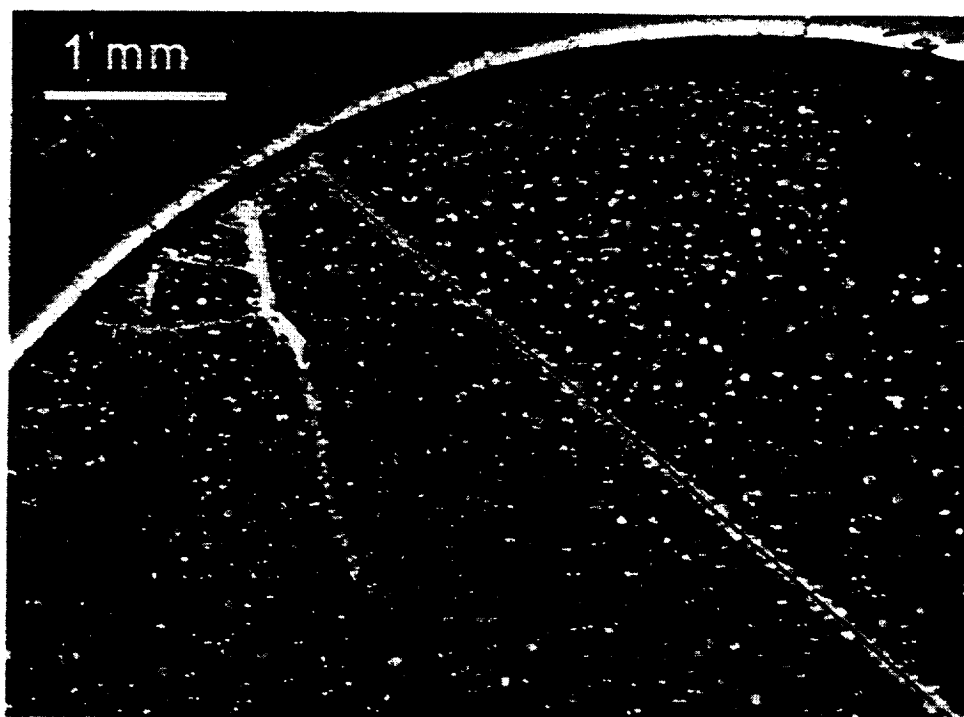


**Figure 4 – Brittle fracture of FEP after x-ray irradiation**





Figure 5 -- Liquid seeping from cracks in FEP induced by x-ray irradiation.

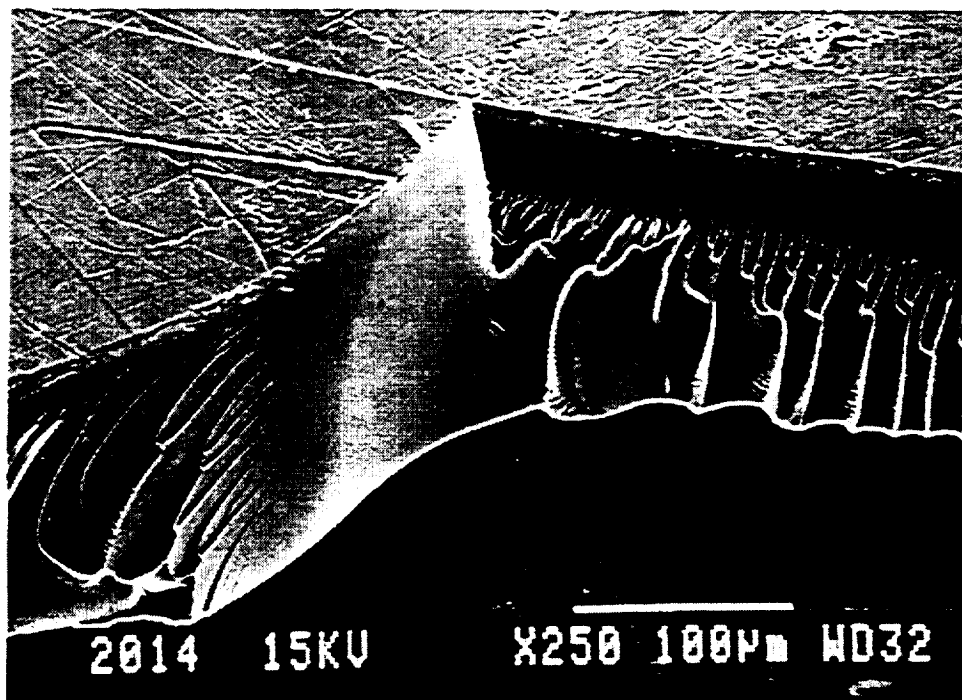
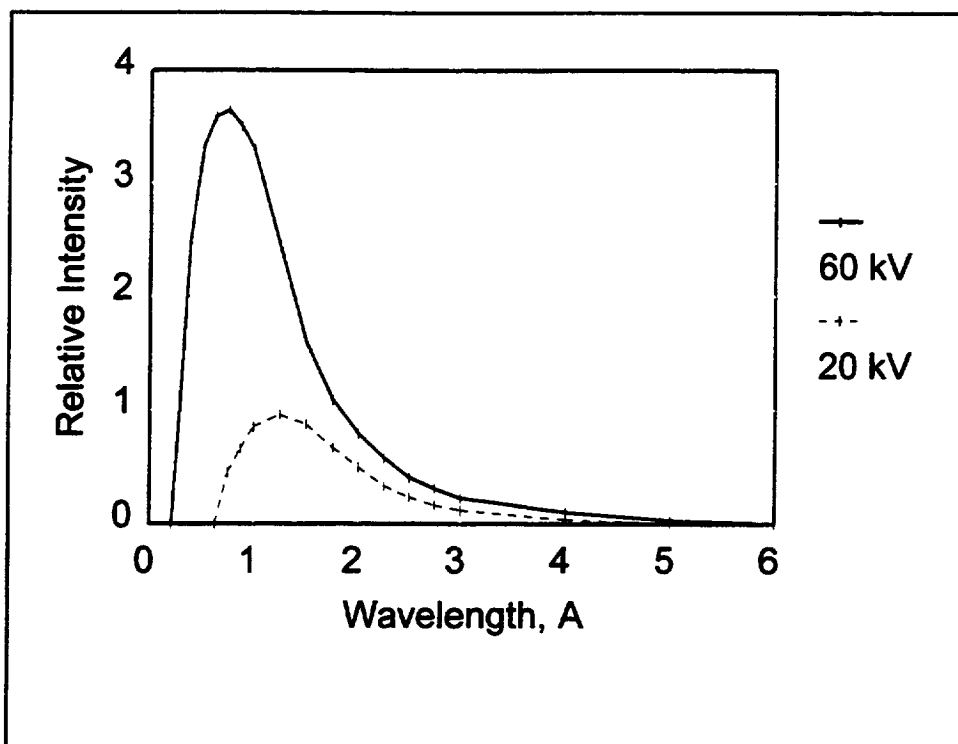
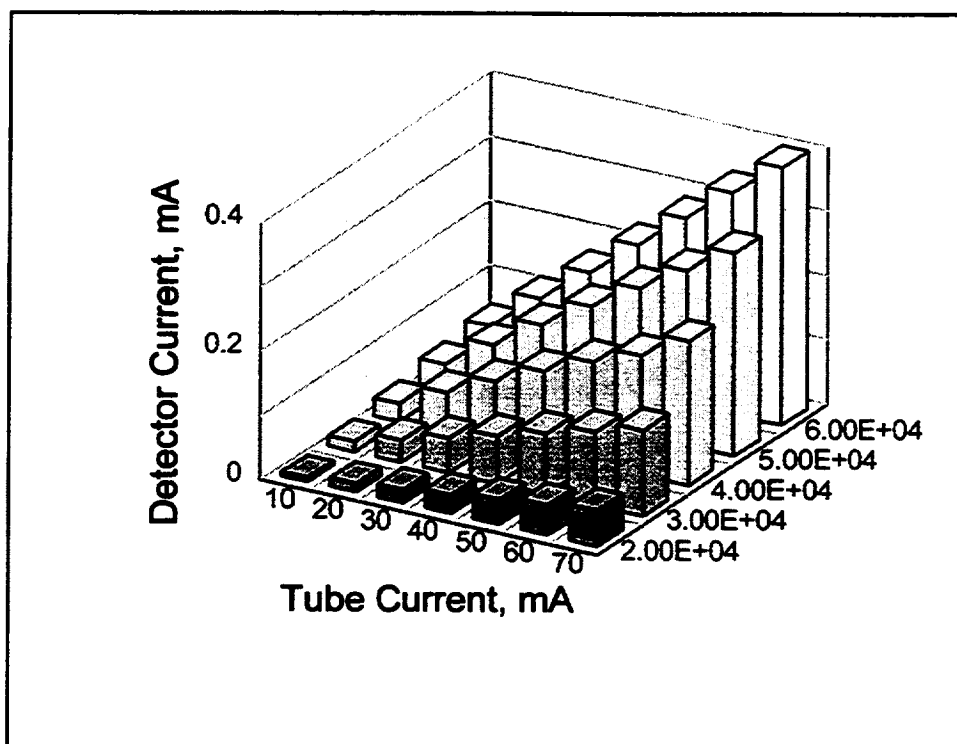


Figure 6 -- Fracture surface of x-ray irradiation induced cracks in FEP.



**Figure 7** – Schematic x-ray spectrum of Bremsstrahlung emitted from a Mo target at excitation potentials of 20 and 60 kV.



**Figure 8** – AXUV detector current as a function of excitation current and voltage of the rotating anode x-ray source.

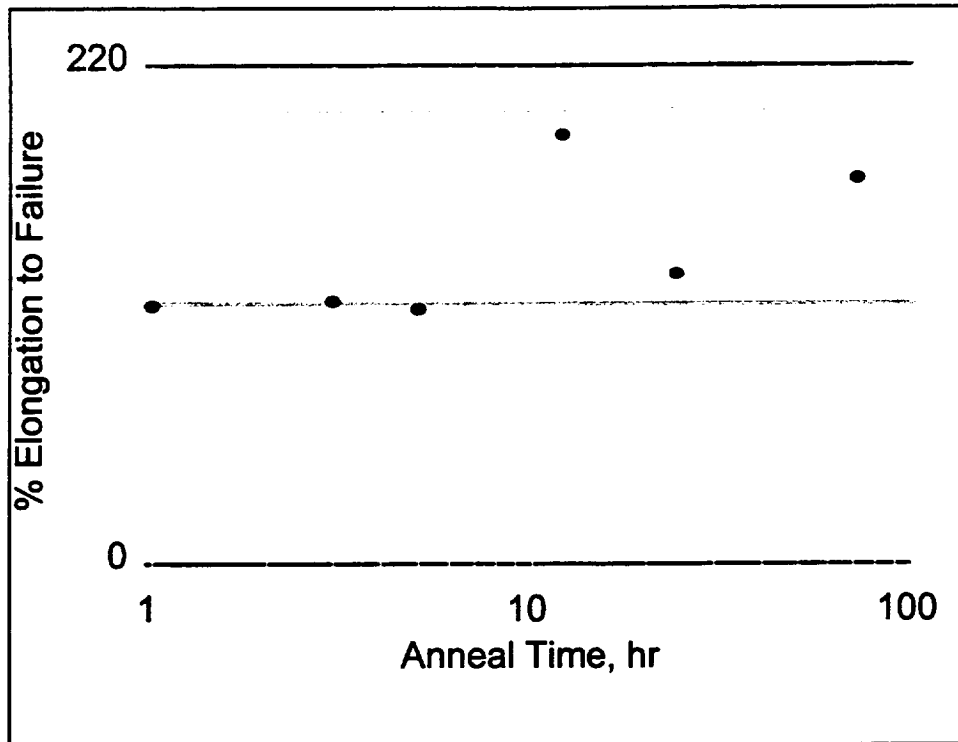


**Figure 9** – Elongation to failure for 5 mil thick aluminized FEP as a function of anneal time in air at 200 °C. Grey lines give mean  $\pm \sigma$  for pristine FEP.

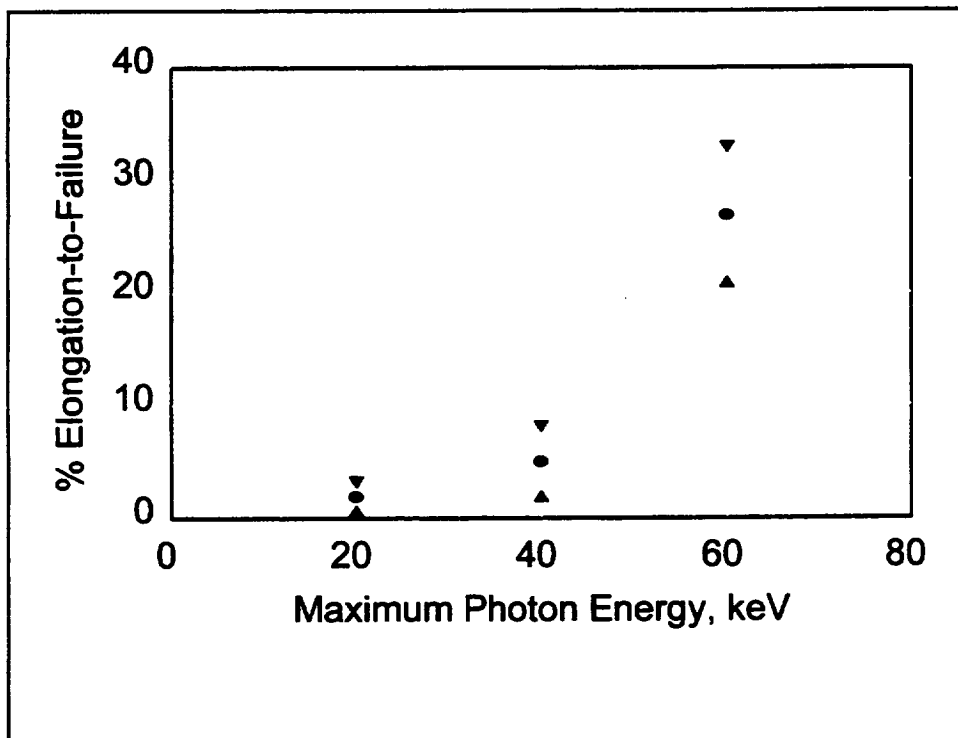


**Figure 10** – Elongation-to-failure for 5 mil thick aluminized FEP exposed to  $10^5$  J/m<sup>2</sup> x-rays of various energies. Mean  $\pm \sigma$  is shown.

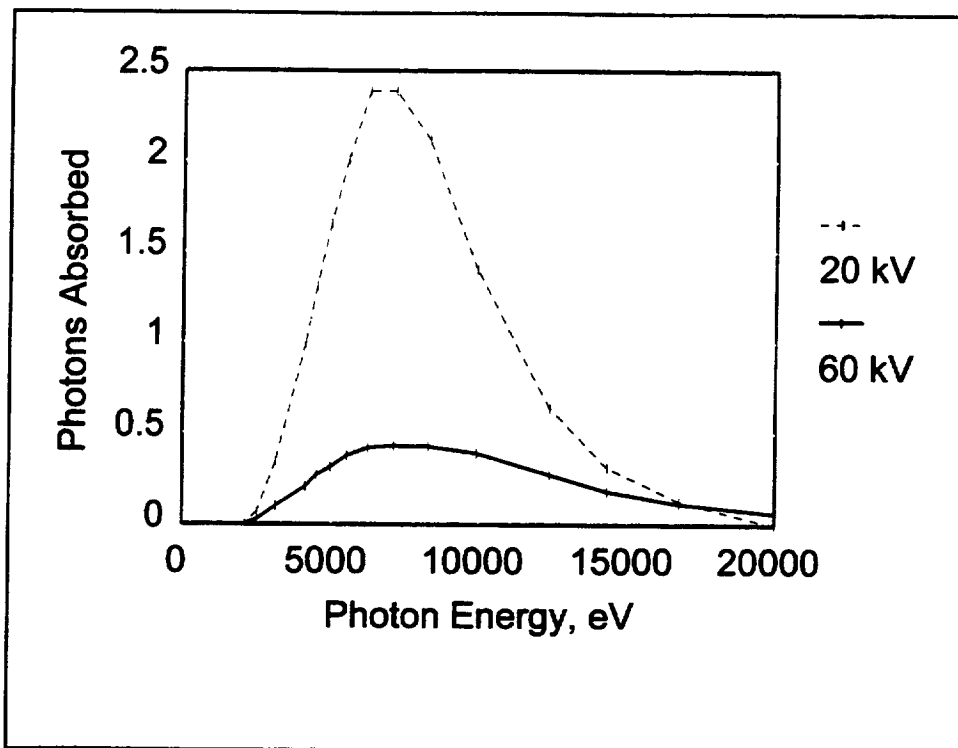


**Figure 11** – Convolution of emission spectrum of x-ray source with absorption spectrum of 5 mil FEP. The absorption on an arbitrary scale.